HHS Public Access

Author manuscript

Clin Cancer Res. Author manuscript; available in PMC 2017 January 15.

Published in final edited form as:

Clin Cancer Res. 2016 January 15; 22(2): 405–414. doi:10.1158/1078-0432.CCR-15-0829.

Sensitivity of KRAS-Mutant Colorectal Cancers to Combination Therapy that Co-Targets MEK and CDK4/6

Elizabeth K. Ziemke[1,2], **Joseph S. Dosch**[1,2], **Joel D. Maust**[1,3], **Amrith Shettigar**[1,2], **Ananda Sen**[4], **Theodore H. Welling**[5], **Karin M. Hardiman**[5], and **Judith S. Sebolt-Leopold**[1,2,3]

[1]Translational Oncology Program, University of Michigan Medical School, Ann Arbor, MI 48109

[2]Department of Radiology, University of Michigan Medical School, Ann Arbor, MI 48109

[3]Department of Pharmacology, University of Michigan Medical School, Ann Arbor, MI 48109

[4]Department of Family Medicine, University of Michigan Medical School, Ann Arbor, MI 48109

[5]Department of Surgery, University of Michigan Medical School, Ann Arbor, MI 48109

Abstract

Purpose—The emerging need for rational combination treatment approaches led us to test the concept that co-targeting MEK and CDK4/6 would prove efficacious in KRAS mutant ($KRAS^{mt}$) colorectal cancers, where upregulated CDK4 and hyperphosphorylated retinoblastoma (RB) typify the vast majority of tumors.

Experimental Design—Initial testing was carried out in the HCT-116 tumor model, which is known to harbor a KRAS mutation. Efficacy studies were then performed with five RB^{+} patient-derived colorectal xenograft models, genomically diverse with respect to KRAS, BRAF, and PIK3CA mutational status. Tolerance, efficacy, and pharmacodynamic evaluation of target modulation were evaluated in response to daily dosing with either agent alone or concurrent co-administration.

Results—Synergy was observed *in vitro* when HCT-116 cells were treated over a broad range of doses of trametinib and palbociclib. Subsequent *in vivo* evaluation of this model showed a higher degree of antitumor activity resulting from the combination compared to that achievable with single agent treatment. Testing of colorectal patient-derived xenograft (PDX) models further

Corresponding author: Judith Sebolt-Leopold, PhD, Translational Oncology Program, University of Michigan, 1600 Huron Parkway, Ann Arbor, MI 48109-2800, Phone (734) 615-7326, jssl@med.umich.edu.

Disclosure of Potential Conflicts of Interest: *The authors declare they have no competing interests.*

Authors's Contributions

Conception and design: Elizabeth K. Ziemke, Joseph S. Dosch, Judith S. Sebolt-Leopold

Development of methodology: Elizabeth K. Ziemke, Joseph S. Dosch, Joel D. Maust, Amrith Shettigar, Judith S. Sebolt-Leopold

Acquisition of data (provided animals, acquired and managed patients, provided facilities, etc.): Elizabeth K. Ziemke, Joseph S. Dosch, Joel D. Maust, Amrith Shettigar, Theodore H. Welling, Karin M. Hardiman, Judith S. Sebolt-Leopold

Analysis and interpretation of data (e.g. statistical analysis, biostatistics, computational analysis): Elizabeth K. Ziemke, Joseph S. Dosch, Ananda Sen, Judith S. Sebolt-Leopold

Writing, review, and/or revision of the manuscript: Elizabeth K. Ziemke, Judith S. Sebolt-Leopold

Administrative, technical, or material support (i.e., reporting or organizing data, constructing database): Elizabeth K. Ziemke, Joseph S. Dosch, Joel D. Maust, Amrith Shettigar, Ananda Sen, Karin Hardiman, Judith S. Sebolt-Leopold

Study supervision: Judith S. Sebolt-Leopold

showed that combination of trametinib and palbociclib was well tolerated and resulted in objective responses in all $KRAS^{mt}$ models tested. Stasis was observed in a KRAS/BRAF wild type and a $BRAF^{mt}$ model.

Conclusions—Combination of trametinib and palbociclib was well tolerated and highly efficacious in all three KRAS mutant CRC PDX models tested. Promising preclinical activity seen here supports clinical evaluation of this treatment approach to improve therapeutic outcome for metastatic colorectal cancer patients.

Introduction

Aberrant hyperactivation of KRAS plays a prominent role in tumor initiation and progression in a broad spectrum of human cancers. KRAS mutations comprise >80% of all RAS mutations and are associated with the highest frequency, roughly 20%, of all human malignancies(1). The incidence of KRAS mutations is especially high in colorectal cancer, where the frequency is >40%. Treatment options for patients with metastatic colorectal cancer (mCRC) harboring a KRAS mutation who have failed first-line chemotherapy are limited, reflected by this disease being the third leading cause of cancer deaths in the United States(2). The monoclonal antibody cetuximab was the first EGFR inhibitor approved for clinical use against mCRC, but provides no benefit to patients whose cancers harbor a KRAS mutation(3,4). Efforts to develop drugs directly targeting mutant KRAS protein remain challenging due to issues with target specificity. Consequently, efforts aimed at pharmacologic intervention of KRAS signaling have focused intensively in recent years on downstream targets in the RAS-MAPK cascade, including BRAF and MEK. Inhibitors of MEK were shown to exert *in vitro* antiproliferative effects in roughly half of the $KRAS^{mt}$ tumors tested (5). However, MEK inhibitors have not shown significant clinical activity in patients with colorectal cancer when used as single agents. Adaptive signaling mechanisms contribute to the failure of MEK inhibitors in a monotherapy setting, dictating the need for rational combination treatment approaches.

The present study was undertaken to explore the therapeutic merits of impairing cell cycle progression by combining agents that target MEK and cyclin-dependent kinase 4 (CDK4). Progression through the G_1-S phase is dependent upon phosphorylation of the retinoblastoma (RB) protein by CDK4 (6) or the highly homologous CDK6 (7). In support of this approach, a synthetic lethal interaction between KRAS and CDK4 has been reported in a mouse model of non-small cell lung carcinoma (8). Furthermore, combined inhibition of MEK and CDK4 was found to elicit significant synergy in NRAS-mutant melanoma, where a gradient model of oncogenic RAS signaling was proposed to explain the observed decoupling of proliferation and survival (9). We believe that there exists a strong scientific rationale for exploration of this combination strategy in colorectal cancer, where RB, the main target of CDK4, is rarely mutated. Inactivation of the *Apc* gene, which is a key early event in colorectal tumorigenesis, is accompanied by upregulation of cyclin D2 along with increased expression of CDK4/6 and hyperphosphorylated Rb(10). A query of cancer microarray databases in Oncomine (http://www.oncomine.org) provides evidence of CDK4 upregulation in colorectal tumors compared to corresponding normal mucosa in 13 out of 37 analyses ($p<0.0001$). Inactivation of p16 via promoter methylation also occurs at a

significant frequency in colorectal tumors (20–50% of cases), resulting in loss of the negative regulatory role of this protein that normally serves as a tumor suppressor to inhibit the assembly of cyclinD-CDK4/6 complexes (11,12). Based on the collective supporting rationale, we hypothesized that dual inhibition of CDK4/6 and MEK is a viable treatment strategy to target the subpopulation of colorectal cancers exhibiting hyperactivated KRAS signaling. Here we report that combined therapy with palbociclib and trametinib did indeed result in tumor regressions in all three $KRAS^{mt}$ patient-derived xenograft models tested. This was achieved with concurrent dosing of both agents at their single agent maximum tolerated doses.

Materials and Methods

Cells

HCT-116 cells were purchased from American Type Culture Collection (ATCC) and were maintained in McCoy's 5A medium with 10% fetal bovine serum (FBS) and 1% Penicillin-Streptomycin-Glutamine (PSG) at 37°C in 5% CO_2.

Drugs

Trametinib was purchased from LC Laboratories (Woburn, MA). Palbociclib was obtained under a Material Transfer Agreement from Pfizer Global R & D. For cellular studies, drugs were dissolved in DMSO at a concentration of 10mM and stock solutions stored at −20°C.

Cell Proliferation Assays

For growth inhibition analysis, cells were seeded in white-walled/clear bottom tissue culture treated 96-well plates at 2000 cells/well and allowed to adhere for 24 hours followed by addition of growth media containing serial dilutions of trametinib, palbociclib, or both drugs in combination. Control wells received DMSO at a final concentration of 0.2%. Cells were incubated for 3 days in the continuous presence of drug or DMSO and viability was measured using CellTiter-Glo (Promega). Viability was calculated as a percentage of the DMSO treated cells. Three replicates were performed for each of the different drug treatment conditions. Data were modeled using a nonlinear regression curve fit with a sigmoidal dose response using GraphPad Prism 5 (GraphPad Software). Synergy calculations were performed using Combenefit software (Cancer Research UK Cambridge Institute).

Patient Samples and Establishment of Patient-Derived Colorectal Xenograft Models

Tumor and matched normal specimens were obtained from patients undergoing liver metastasectomies or colon resections of primary disease at the University of Michigan University Hospital (Ann Arbor, MI). All patients provided informed written consent and samples were procured with approval of the University of Michigan Institutional Review Board (HUM00065489). Specimens were obtained within four hours of surgery and immediately transferred to DMEM/F12 media supplemented with 10% fetal bovine serum and 1% Penicillin-Streptomycin-Glutamine at 4°C. A portion of normal colon specimens were fixed in 10% neutral buffered formalin (NBF) and the remainder snap frozen in liquid nitrogen. Portions of tumor specimens were either fixed in 10% NBF, snap frozen in liquid

nitrogen, or divided into fragments approximately 3 × 3 mm for subcutaneous implantation into female 6–7 week old CIEA NOG mice (NOD.Cg-Prkdcscid Il2rgtm1Sug/JicTac from Taconic) using an 11G Trocar needle. Tumor-implanted mice were monitored for tumor growth for up to four months following implantation. Xenografted tumors from the NOG mice were passaged into female 6–7 week old NCR nude mice (CrTac:NCr-Foxn1nu from Taconic) for model expansion. PDX models were maintained in nude mice for no more than four passages before fresh material from the freezer was used to regenerate the line.

Xenograft Studies

Female 6–7 week old NCR nude mice (CrTac:NCr-*Foxn1*^{nu} from Taconic), 6–7 weeks old, were implanted subcutaneously with low passage PDX tumor fragments (˜30mg) into the region of the right axilla. Mice were randomized into treatment groups and treatments initiated when tumors reached 100 to 200mg. Trametinib and palbociclib were administered daily for 10 to 14 days by oral gavage as a fine suspension in 0.5% HPMC with 0.2% Tween80 or saline, respectively, based upon individual animal body weight (0.2ml/20g). Subcutaneous tumor volume and body weights were measured two to three times a week. Tumor volumes were calculated by measuring two perpendicular diameters with calipers and using the formula: tumor volume = (length × width^2)/2. Mice were held following cessation of treatment until tumor burdens reached ˜1000mg, to allow for calculation of tumor growth delay. Percent treated/control (%T/C) was calculated by dividing the median treated tumor weight by the median control tumor weight and multiplying by 100 on the last day of treatment. Tumor growth delay (T-C) was calculated by subtracting the median time to reach evaluation size (750mg) of the treated group by the median time to evaluation size of the control group. A partial regression (PR) is defined as a tumor that regressed to <= 50% of the baseline tumor volume. A complete response (CR) is defined as a tumor below the limits of palpation (≤40 mg). All procedures related to the handling, care, and treatment of animals was conducted in accordance with University of Michigan's Committee on the Use and Care of Animals guidelines.

Mutation Detection

Initial mutational screening was performed using the qBiomarker™ Somatic Mutation PCR Array for Human Colon Cancer (Qiagen). Mutational status was confirmed by Sanger sequencing.

Flow Cytometry

For cell cycle experiments, HCT-116 cells were seeded into 6 well plates at 300,000 cells/well and allowed to settle overnight. Cells were treated with either DMSO (0.1%), trametinib (10 nM), palbociclib (1 μM) or combination of the two agents at these concentrations for 24 hr. Cells were harvested with 0.05% Trypsin, spun down, washed with PBS, fixed with 70% ethanol and stored at 4°C for at least 24 hr. Once ready for analysis, the fixed cells were spun down, washed with PBS, and allowed to incubate for 30 minutes prior to analysis with a propidium iodide solution: 50 μg/ml propidium iodide (Life Technologies, P3566), 0.1% Triton X-100 (Sigma-Aldrich, T9284), 50 μg/ml RNase A (Qiagen, 1007885) and PBS. Data were collected on a Cyan ADP Analyzer (Beckman

Coulter), with collection of 10,000 events. Histograms were generated and cell cycle analyses were performed using flow cytometry analysis software ModFit LT V4.0.5 (Verity Software House).

p16 Promoter Methylation

Following bisulfite conversion of genomic DNA, a methylation-specific PCR (MSP) assay was carried out as described by Herman *et al* (13). MSP using primers selectively recognize a fully methylated/unmethylated sequence in the promoter region of p16 that contains numerous CpG islands. A fully methylated control (enzymatically methylated human MLH1 mismatch repair gene) was probed in every assay in order to ensure bisulfite conversion fidelity.

Western Blotting

Tumors were manually homogenized with a Teflon pestle (Bel-Art) in lysis buffer [25 mmol/L Tris-HCl (pH 7.6), 150 mmol/L NaCl, 1% Nonidet P-40, 10% glycerol, 1 mM EDTA1 mmol/L dithiothreitol (DTT), and protease and phosphatase inhibitors, rocked for 30 minutes at 4°C, and centrifuged at 14,000 rpm for 210 min at 4°C. Protein concentration was determined by BioRad Protein Assays and lysates were subsequently subjected to SDS gel electrophoresis. Proteins were transferred to polyvinylidene fluoride (PVDF) membranes and probed with primary antibodies recognizing p-ERK1/2 (thr202/tyr204), ERK1/2, p-RB (ser780), and RB (all from Cell Signaling Technology) and GAPDH (Abcam). After incubation with anti-rabbit HRP linked secondary antibody (Jackson ImmunoResearch Laboratories, Inc.), proteins were detected using chemiluminescence (GE Healthcare).

Immunohistochemistry

Tissues were fixed in 10% neutral buffered formalin, embedded in paraffin, and sectioned in accordance with standard procedures. Embedding, sectioning, hematoxylin and eosin (H&E), and all other staining was performed by the University of Michigan Cancer Center Histopathology Core. The Ki67, pRb, and cleaved caspase-3 antibodies for IHC were obtained from Cell Signaling Technology and the total RB antibody for IHC from Abcam. Images were taken with a Nikon E-800 microscope, Olympus DP71 digital camera, and DP Controller software. For quantification of staining, representative images were obtained from the stained slides at ×40 objective magnification for ImmunRatio analysis. For each treatment condition (vehicle, trametinib, palbociclib and combination), five representative fields of view from four individual tumors were analyzed. The images were analyzed using the basic mode in the ImmunoRatio software. Quantification is presented as mean ± SEM. In assessing two different groups, two-tailed Student's *t* test (unpaired) was used for statistical analysis.

Statistical Analysis of PDX Efficacy Studies

ANOVA was applied on the outcomes of tumor volume and the time to reach a tumor burden of 750 mg under the log-normal assumption. This was followed by post-hoc pairwise comparison with Bonferroni adjusted significance threshold set at P = .05/6 = .008, accounting for the six possible pairwise differences. Tumor growth delay data (time for

tumors to reach 750mg) for the CRM 13-180 study was analyzed using censored log-normal data since roughly 15% of the values were right censored in the sense that tumor volume did not reach 750 mg at the time the animals were sacrificed. P values indicating statistical significance are provided in the figure legends.

Results

Evaluation of toxicity of trametinib and palbociclib in combination

Informed selection of agents is crucial for exploring the central hypothesis that dual targeting of MEK and CDK4/6 holds therapeutic promise for the treatment of $KRAS^{mt}$ CRC. We selected palbociclib to inhibit CDK4/6 activity based on its known ability to selectively target these kinases (14) and its promising clinical activity in breast cancer patients that has led to its regulatory approval. A multitude of MEK inhibitors are available with proven ability to effectively impair ERK activation *in vivo* (15). The potential for overlapping toxicities when combining palbociclib and the MEK inhibitor PD0325901 proved problematic in early work carried out to evaluate MEK inhibitor-based combinations (Sebolt-Leopold, unpublished data). However, we found that trametinib at its reported single agent MTD of 3 mg/kg (16) can be administered for a full course of 10 daily treatments in combination with palbociclib administered daily at its single agent MTD (150 mg/kg) with weight loss in the combination group never surpassing 10% (Supplementary Figure 1). The absence of overlapping toxicities upon combination of these two agents at their reported single agent maximum tolerated doses provided the basis for subsequent pharmacological evaluation of this approach.

Synergy of trametinib and palbociclib combination therapy in HCT-116 model

To explore the therapeutic potential of combining trametinib and palbociclib to treat $KRAS^{mt}$ CRC, we first carried out studies with the HCT-116 CRC cell line, which carries an activating KRAS mutation (G13D), and is conducive to evaluating the correlation of *in vitro* to *in vivo* data for predicting sensitivity. A 5 × 5 matrix combination dose response screen of trametinib and palbociclib was performed in HCT-116 cells to assess both single agent activity and evaluate additive, synergistic or antagonistic interactions across a range of doses. As single agents alone, both trametinib and palbociclib exhibited dose-dependent anti-proliferative activity with IC_{50}'s of 5.7 nM and 5.9 μM, respectively (data not shown). A heat map of the excess over highest single agent (EOHSA) is shown depicting the doses at which the drug combinations achieve better than predicted inhibition of cell viability (Figure 1A, top panel). The combination of trametinib and palbociclib was synergistic over the majority of dose combinations tested. Additional synergy evaluation was performed by calculating the combination index (CI) values based on the median effect principle (17). Consistent with the EOHSA method, we observed synergy at the majority of doses tested, and importantly at doses that are thought to be clinically relevant (Figure 1A, bottom panel).

Subsequent *in vivo* evaluation of HCT-116 tumor-bearing mice provided additional evidence that this drug combination produced a higher degree of antitumor activity than that achievable from single agent treatment. Combination treatment with trametinib and palbociclib resulted in a 14-day tumor growth delay (Fig. 1B), which was significantly

longer than the 7-day tumor growth delay elicited from either single agent alone (7 days in each case). Treatment with the combination also resulted in partial tumor regressions in two of five mice, whereas single agent treatment resulted in no objective responses.

Trametinib and palbociclib combination therapy potentiates G1 arrest

To characterize the mechanism of growth inhibition incurred in response to trametinib and palbociclib combination therapy, cell cycle distribution studies were carried out. After 24h of treatment, a significant increase in the percentage of HCT-116 cells arrested in G0/G1 was found to occur in response to inhibition of both MEK and CDK4/6 (Figure 1C). As expected, treatment with trametinib or palbociclib alone led to a G1 block (61–66% compared to 35% of DMSO treated cells). Combination of the two agents led to 84% of cells being arrested in G1 and was accompanied by decreases in the percentages of cells in S and G2-M.

Patient-derived colorectal xenografts commonly are positive for phosphorylated RB expression

A heterogeneous panel of patient-derived CRC xenograft (PDX) models was established from fresh biospecimens procured from patient surgeries (Supplementary Table 1). Of the eighteen PDX models established, eleven originated from colon resections, six resulted from liver metastasectomies, and one was established from an ovarian metastasis. Both the original patient tissue and the xenograft tissue were analyzed by H&E staining, whereupon CRC PDX tissues were found to exhibit a similar histological phenotype to that of patient tissue from which they were derived (Figure 2A). Genomic profiling revealed that the most prevalent oncogenic mutations occur in KRAS, PIK3CA, and BRAF as reflected by incidence rates of 44%, 22%, and 11%, respectively. Overall, the frequency of these mutations in our panel is consistent to that reported in the clinical CRC population. Targeted exome sequencing was also carried out comparing the genomic profile of the xenograft tumors to the original patient samples. In each case, no difference in the major oncogenic drivers was found between these two sets of samples (data not shown). This suggests that our panel is indeed an accurate representation of clinically-relevant disease.

When analyzed for pRB expression, all eighteen models were found to be RB positive (Supplementary Figure 2). Five of these models (Table 1) were selected on the basis of diverse genotypes to explore the *in vivo* consequences of combined MEK and CDK4/6 inhibition: three models that are $KRAS^{mt}$, one model that is $BRAF^{mt}$ and a fifth model that is $BRAF^{WT}KRAS^{WT}$. All five models were characterized for expression levels of CDK4, pERK, and pRB compared to matching normal tissue from the same patient from whom the tumor specimen originated. Normal tissue was not available for the CRM 12-1159 model, since it originated from a patient undergoing hepatic metastasectomy. As shown in Figure 2B, there were no discernable differences in CDK4 and pERK expression among this subset of PDX models when comparing tumor models to each other or to normal tissue. This result is not surprising in light of the high proliferation rate of normal epithelial tissue in the gut. Comparative immunohistochemical staining for pRB expression in these five models is shown in Figure 2C. Total Rb expression immunochemistry is shown in Supplementary Figure 3. Quantitation of pRB staining of multiple slides revealed that the percentage of

positive-stained cells in normal tissue generally did not vary, ranging from 2.7% to 5.6%. A greater range in pRB expression was found in the individual tumor models as reflected by values of 23.8% (CRM 12-1159), 17.4% (CRM 13-180), 8.0% (CRC 13-983), 4.2% (CRC 13-1333), and 6.2% (CRC 14-136).

Analysis of the methylation status of p16 was also analyzed in our models, revealing that none of the three $KRAS^{mt}$ models exhibited methylation of p16. Only the $BRAF^{mt}$ model showed evidence of p16 methylation (Supplementary Figure 4).

The combination of trametinib and palbociclib is efficacious in $KRAS^{mt}$ patient-derived CRC xenografts

The three $KRAS^{mt}$ CRC PDX models advanced for pharmacological evaluation were selected on the basis of diverse genotypes ($KRAS^{G12V}$ $PIK3CA^{WT}$, $KRAS^{G12D}$ $PIK3CA^{Q546L}$, and $KRAS^{Q61H}$ $PIK3CA^{E542K}$). Subcutaneous tumors of these three models (CRM 13-180, CRC 13-1333, and CRC 14-136) were implanted into NCR nude mice. Treatment was initiated when the mean tumor volume reached ~150 mm^3. For each model, administration of the single agents was modestly inhibitory as reflected by tumor growth inhibition (% T/C) values that ranged from 29–72% for trametinib and 41–72% for palbociclib (Figure 3A, Table 2). Single agent treatment resulted in tumor growth delay values that were also not significant when compared to the vehicle control group. As anticipated, the two PIK3CA mutated models were more refractory to trametinib treatment alone than the $PIK3CA^{WT}$ model. Combination treatment resulted in enhanced tumor growth inhibition (% T/C 17–29%) in all three models. Very importantly, objective responses were seen in all three $KRAS^{mt}$ models treated with the combination (Table 2, Figure 3B). Whereas stable disease or progression was observed for the single agent cohorts, partial regressions were observed in the combination groups in all three models. Intragroup variability in the combination groups was generally quite low as reflected by SEM values that ranged from 6 to 21%. Statistically significant tumor growth delay was observed in two of the models (20 and >90 days for CRC 13-1333 and CRM 13-180 models, respectively). However, the response of CRC 14-136 tumors to combination treatment was clearly less durable compared to the other two $KRAS^{mt}$ models as reflected by resumption of tumor growth as soon as treatment was terminated. Importantly, efficacy derived from the combination of trametinib and palbociclib at their respective single agent MTD doses was not accompanied by any apparent adverse clinical signs of toxicity. The maximum amount of treatment-related weight loss in the combination group did not exceed 10%, consistent with earlier toxicity testing carried out in non-tumor bearing animals (Supplementary Figure 5).

The combination of trametinib and palbociclib potentiates suppression of RB phosphorylation

Pharmacodynamic evaluation of pERK and pRb expression levels revealed significant target modulation by each agent. Representative data are shown in Figure 4 for the CRM 13-180 tumor model as measured by immunoblotting (Figure 4A) and immunohistochemistry (Figure 4B). Total Rb and ERK expression levels are shown in Supplementary Figure 6. Interestingly, tumors from the animals in the combination arm exhibited a significant

reduction in pRB levels compared to palbociclib treatment alone, consistent with enhanced antitumor activity as well as reduced Ki67 staining in this group (Figure 4C). Immunohistochemical staining of cleaved caspase-3 revealed no induction of apoptosis in any of the four experimental groups (Supplementary Figure 7).

Trametinib and palbociclib combination treatment of KRAS wild type and BRAF mutant PDX models is not superior to palbociclib monotherapy

The effectiveness of this combination treatment strategy was additionally tested in two CRC PDX models that are wild type with respect to RAS. Chosen for study were the CRM 12-1159 model, which harbors a PIK3CA mutation, and CRC 13–893, which is a BRAF mutant model. As summarized in Table 2, CRM 12-1159 tumors proved to be refractory to MEK inhibitor single agent treatment as reflected by both T/C and T-C parameters (72% and 3 day, respectively). Growth of this KRAS/BRAF wild type model was modestly impaired by CDK4/6 inhibitor single agent treatment, with T/C and T-C values of 45% and 16 days, respectively. Furthermore, the combination of trametinib and palbociclib did not elicit a meaningful increase in therapeutic activity compared to palbociclib alone against CRM 12-1159 tumors, as reflected by comparable or equivalent activity parameters among the two groups.

The combination of these two agents was also not superior to palbociclib alone when treating BRAF mutant CRC 13-983 tumors (23 day versus 25 day growth delay for the combination and palbociclib single agent groups, respectively). However, CRC 13–893 tumors were notably more responsive to both trametinib and palbociclib as single agents than all other models tested, including the KRAS mutant models. Whereas no objective responses were observed with CRM 12-1159 and CRC 13-983 tumors in any of the treatment arms, combination treatment with trametinib and palbociclib did appear to lead to stasis (Table 2, Figure 3A).

DISCUSSION

Since the introduction of the first orally active MEK inhibitor CI-1040 into clinical trials, the anticancer drug potential of this target class has been intensely investigated (15,18,19). A number of research programs were subsequently launched around the CI-1040 template in efforts to optimize the pharmacologic properties of this mechanistic class of molecular targeted agents. Trametinib emerged as the first MEK inhibitor to win regulatory approval for the treatment of metastatic $BRAF^{mt}$ melanoma (20). However, MEK inhibitors as a target class have not shown demonstrable clinical activity in patients with colorectal cancer when used as single agents. This result is not unexpected based on preclinical studies showing tumor stasis at best against $KRAS^{mt}$ tumors, likely reflecting the limitations of single agent-targeted approaches for colorectal cancer.

Reactivation of CRAF has been reported to limit the ability of MEK inhibitors to inhibit ERK signaling in KRAS mutant tumors that arises from the induction of RAF-MEK complexes (21). Activated ERK feedback serves to impair signaling through the RAF/MEK/ERK pathway in $KRAS^{mt}$ cells by directly phosphorylating and inhibiting CRAF kinase activity (22). Consequently, release of feedback inhibition of CRAF kinase

activity results in induction of MEK phosphorylation. However, Lito *et al* showed that not all allosteric MEK inhibitors behave similarly; newer agents like trametinib act to target catalytic activity of MEK and further impair its reactivation by CRAF by disrupting RAF-MEK complexes (21). They further showed that trametinib was less affected than PD0325901 to reactivated CRAF signaling, suggesting that it results in more durable inhibition of ERK signaling by increasing the dissociation rate of MEK from RAF, an important feature when targeting $KRAS^{mt}$ tumors. Based on these considerations, trametinib emerged from the multitude of MEK inhibitors currently available as a strong candidate for inclusion in combination treatment studies.

Exome sequencing conducted on a large population of patients diagnosed with CRC showed that the G1-S checkpoint is genetically altered in approximately half of these cases (23). Consequently, this subpopulation of $KRAS^{mt}$ colorectal cancer patients emerge as potential candidates for dual targeting of CDK4/6 and MEK. Along these lines, data reported here provide further support for this combination approach, as co-targeting these kinases led to a significant increase in $KRAS^{mt}$ CRC cells arrested in G0/G1 compared to either single targeted approach.

First, we felt it important to address the potential for overlapping toxicities when combining trametinib with a CDK4/6 inhibitor. We have found that other MEK inhibitors, namely PD0325901 and binimetinib, required dose lowering of their respective maximum tolerated doses when they were co-administered with palbociclib (data not shown). Here we report that trametinib at its single agent MTD could be administered for a full course of 10–14 daily treatments in combination with palbociclib, also administered daily at its single agent MTD. We are not suggesting that other MEK inhibitors do not possess therapeutic potential in combination with palbociclib. Rather, the present study provides support for broader testing of the MEK/CDK4/6 combination concept in CRC with the portfolio of agents available against both of these molecular targets. In this regard, it is encouraging that binimetinib in combination with the CDK4/6 inhibitor LEE011 has shown hints of early clinical activity in patients with NRAS-mutant melanoma (24).

Clinical application of this combination approach in the CRC population needs to address the multi-RAS signatures of colorectal cancer. While the majority of KRAS mutations occur within exon 2 at codons 12 or 13, activating mutations can also occur in exon 3 or 4 at codons 61 and 146. With an incidence rate that is considerably lower (1–4%) than those in exon 2, these mutations as well as those of NRAS are also negative predictive biomarkers for anti-EGFR therapy (4,25). It is encouraging that the combination of trametinib and palbociclib proved efficacious against a $KRAS^{mt}$ PDX model mutated in codon 61 (UM CRC 14-136), as reflected by a T/C value of 29% on the last day of treatment. However, these tumors quickly re-grew after treatment was terminated and did not result in a statistically significant tumor growth delay. Additional testing of codon 61 or 146 $KRAS^{mt}$ models is warranted to further explore the therapeutic potential of this combination strategy against this rare subpopulation of CRC tumors.

One of the major obstacles to successful deployment of MEK inhibitors to treat $KRAS^{mt}$ CRC is the high frequency of PIK3CA mutations that occur in these tumors. These

mutations serve to restore cyclin D1 expression and cell cycle progression causing them to no longer be dependent on KRAS/MEK/ERK signaling (26). Major efforts have been expended in recent years to combine MEK and PI3K pathway inhibitors in the clinic only to be met with significant toxicity issues. Combination of MEK and PI3K inhibitors was further shown to result in disappointing activity in RAS^{mt} CRC PDX models as evidenced by disease stabilization but absence of overt tumor regression (27). Since virtually all CRC tumors are RB^{+}, an alternative strategy for blocking cell cycle progression in $PIK3CA^{mt}$ tumors is to incorporate a CDK4/6 inhibitor in the treatment regimen. We report here that the CDK4/6 inhibitor palbociclib does in fact render MEK inhibitor-insensitive CRC PDX models sensitive to this combination treatment strategy in all three $KRAS^{mt}$ models evaluated, two of which are also $PI3KCA^{mt}$. It is noteworthy that the HCT-116 model, which we earlier showed to be highly sensitive to the trametinib/palbociclib combination, also harbors a PIK3CA mutation (H1047R). These results have important implications for future clinical testing of this combination treatment strategy in patients diagnosed with $KRAS^{mt}$ CRC, for which there exists marginally effective therapies. It is especially encouraging that the combination of trametinib and palbociclib elicited tumor regressions in all of these models at doses that did not produce any weight loss for the duration of treatment.

Two PDX models were included in our analyses that are KRAS wild type, one of which was BRAF mutated (V600E). While the trametinib/palbociclib combination proved less effective in these models compared to its activity against $KRAS^{mt}$ tumors, we were nonetheless surprised to observe stasis. Further investigation of additional KRAS wild type and $BRAF^{mt}$ models is warranted to understand the significance of this early finding.

In conclusion, we have identified a promising combination strategy, namely dual targeting of MEK and CDK4/6, that merits consideration for clinical testing. Our data with patient-derived xenograft models additionally suggest that patients with coexistent PIK3CA mutations are candidates for this combination treatment strategy directed against $KRAS^{mt}$ cancer. Further mouse trials are warranted with an expanded CRC PDX panel to capture the heterogeneity encountered in the clinic to optimize clinical trial design and further define a patient enrichment strategy.

Supplementary Material

Refer to Web version on PubMed Central for supplementary material.

Acknowledgments

We wish to thank Pfizer Global R & D for supplying palbociclib to carry out these studies.

Grant Support: This work was supported by grants from the NIH (GI SPORE P50 CA130810 to J.S. Leopold; R01 CA155198 to J.S. Leopold).

Abbreviations

CRC	colorectal cancer

PDX patient-derived xenograft

References

1. Baines AT, Xu D, Der CJ. Inhibition of Ras for cancer treatment: the search continues. Future Med Chem. 2011; 3(14):1787–808. [PubMed: 22004085]
2. Jemal A, Bray F, Center MM, Ferlay J, Ward E, Forman D. Global cancer statistics. CA Cancer J Clin. 2011; 61(2):69–90. [PubMed: 21296855]
3. Lievre A, Bachet JB, Le Corre D, Boige V, Landi B, Emile JF, et al. KRAS mutation status is predictive of response to cetuximab therapy in colorectal cancer. Cancer Res. 2006; 66(8):3992–5. [PubMed: 16618717]
4. Loupakis F, Ruzzo A, Cremolini C, Vincenzi B, Salvatore L, Santini D, et al. KRAS codon 61, 146 and BRAF mutations predict resistance to cetuximab plus irinotecan in KRAS codon 12 and 13 wild-type metastatic colorectal cancer. Br J Cancer. 2009; 101(4):715–21. [PubMed: 19603018]
5. Wee S, Jagani Z, Xiang KX, Loo A, Dorsch M, Yao YM, et al. PI3K pathway activation mediates resistance to MEK inhibitors in KRAS mutant cancers. Cancer Res. 2009; 69(10):4286–93. [PubMed: 19401449]
6. Lundberg AS, Weinberg RA. Functional inactivation of the retinoblastoma protein requires sequential modification by at least two distinct cyclin-cdk complexes. Mol Cell Biol. 1998; 18(2): 753–61. [PubMed: 9447971]
7. Meyerson M, Harlow E. Identification of G1 kinase activity for cdk6, a novel cyclin D partner. Mol Cell Biol. 1994; 14(3):2077–86. [PubMed: 8114739]
8. Puyol M, Martin A, Dubus P, Mulero F, Pizcueta P, Khan G, et al. A synthetic lethal interaction between K-Ras oncogenes and Cdk4 unveils a therapeutic strategy for non-small cell lung carcinoma. Cancer Cell. 2010; 18(1):63–73. [PubMed: 20609353]
9. Kwong LN, Costello JC, Liu H, Jiang S, Helms TL, Langsdorf AE, et al. Oncogenic NRAS signaling differentially regulates survival and proliferation in melanoma. Nat Med. 2012; 18(10): 1503–10. [PubMed: 22983396]
10. Cole AM, Myant K, Reed KR, Ridgway RA, Athineos D, Van den Brink GR, et al. Cyclin D2-cyclin-dependent kinase 4/6 is required for efficient proliferation and tumorigenesis following Apc loss. Cancer Res. 2010; 70(20):8149–58. [PubMed: 20736363]
11. Esteller M, Gonzalez S, Risques RA, Marcuello E, Mangues R, Germa JR, et al. K-ras and p16 aberrations confer poor prognosis in human colorectal cancer. J Clin Oncol. 2001; 19(2):299–304. [PubMed: 11208819]
12. Ogino S, Nosho K, Kirkner GJ, Kawasaki T, Meyerhardt JA, Loda M, et al. CpG island methylator phenotype, microsatellite instability, BRAF mutation and clinical outcome in colon cancer. Gut. 2009; 58(1):90–6. [PubMed: 18832519]
13. Herman JG, Graff JR, Myohanen S, Nelkin BD, Baylin SB. Methylation-specific PCR: a novel PCR assay for methylation status of CpG islands. Proc Natl Acad Sci U S A. 1996; 93(18):9821–6. [PubMed: 8790415]
14. Fry DW, Harvey PJ, Keller PR, Elliott WL, Meade M, Trachet E, et al. Specific inhibition of cyclin-dependent kinase 4/6 by PD0332991 and associated antitumor activity in human tumor xenografts. Mol Cancer Ther. 2004; 3(11):1427–38. [PubMed: 15542782]
15. Zhao Y, Adjei AA. The clinical development of MEK inhibitors. Nat Rev Clin Oncol. 2014; 11(7): 385–400. [PubMed: 24840079]
16. Gilmartin AG, Bleam MR, Groy A, Moss KG, Minthorn EA, Kulkami SG, et al. GSK1120212 (JTP-74057) is an inhibitor of MEK activity and activation with favorable pharmacokinetic properties for sustained in vivo pathway inhibition. Clin Cancer Res. 2011; 17(5):989–1000. [PubMed: 21245089]
17. Chou T. Drug combination studies and their synergy quantification using the Chou-Talalay method. Cancer Res. 2010; 70(2):440–6. [PubMed: 20068163]

18. Sebolt-Leopold JS, Dudley DT, Herrera R, Van Becelaere K, Wiland A, Gowan RC, et al. Blockade of the MAP kinase pathway suppresses growth of colon tumors in vivo. Nat Med. 1999; 5(7):810–6. [PubMed: 10395327]
19. Lorusso PM, Adjei AA, Varterasian M, Gadgeel S, Reid J, Mitchell DY, et al. Phase I and pharmacodynamic study of the oral MEK inhibitor CI-1040 in patients with advanced malignancies. J Clin Oncol. 2005; 23(23):5281–93. [PubMed: 16009947]
20. Wright CJM, McCormack PL. Trametinib: first global approval. Drugs. 2013; 73:1245–54. [PubMed: 23846731]
21. Lito P, Saborowski A, Yue J, Solomon M, Joseph E, Gadal S, et al. Disruption of CRAF-mediated MEK activation is required for effective MEK inhibition in KRAS mutant tumors. Cancer Cell. 2014; 25(5):697–710. [PubMed: 24746704]
22. Dougherty MK, Muller J, Ritt DA, Zhou M, Zhou XZ, Copeland TD, et al. Regulation of Raf-1 by direct feedback phosphorylation. Mol Cell. 2005; 17:215–24. [PubMed: 15664191]
23. Yu J, Wu WKK, Li X, He J, Li XX, Ng SSM, et al. Novel recurrently mutated genes and a prognostic mutation signature in colorectal cancer. Gut. 2015; 64(4):636–45. [PubMed: 24951259]
24. Sosman JA, Kittaneh M, Lolkema MP, Postow MA, Schwartz G, Franklin C, et al. A phase Ib/2 study of LEE011 in combination with binimetinib (MEK162) in patients with NRAS-mutant melanoma: Early encouraging clinical activity. J Clin Oncol. 2014; 32:5s. (suppl: abstr 9009).
25. Douillard JY, Oliner KS, Siena S, Tabernero J, Burkes R, Barugel M, et al. Panitumumab-FOLFOX4 treatment and RAS mutations in colorectal cancer. N Engl J Med. 2013; 369(11):1023–34. [PubMed: 24024839]
26. Halilovic E, She QB, Ye Q, Pagliarini R, Sellers WR, Solit DB, et al. PIK3CA mutation uncouples tumor growth and cyclin D1 regulation from MEK/ERK and mutant KRAS signaling. Cancer Res. 2010; 70(17):6804–14. [PubMed: 20699365]
27. Migliardi G, Sassi F, Torti D, Galimi F, Zanella ER, Buscarino M, et al. Inhibition of MEK and PI3K/mTOR suppresses tumor growth but does not cause tumor regression in patient-derived xenografts of RAS-mutant colorectal carcinomas. Clin Cancer Res. 2012; 18(9):2515–25. [PubMed: 22392911]

Translational Relevance

Activating mutations in the RAS/RAF/MEK pathway present a therapeutic challenge to clinical management of a broad spectrum of solid tumors, including colorectal cancers. Despite advancement of a multitude of MEK inhibitors into clinical trials, they have failed to elicit sufficient activity to significantly impact outcome in patients with metastatic colorectal cancer, thus dictating the need for rational combination treatment approaches. We demonstrate that the CDK4/6 inhibitor palbociclib may have great promise beyond breast cancer as it leads to improved therapeutic outcome when combined with the MEK inhibitor trametinib to treat patient-derived colorectal xenografts. We describe efficacy testing of five heterogeneous colorectal cancers and report that the $KRAS^{mt}$ subset was most responsive to this combination strategy. Promising preclinical activity seen here suggest that dual inhibition of MEK and CDK4/6 is a viable treatment strategy to target the subpopulation of colorectal cancers exhibiting hyperactivated KRAS signaling.

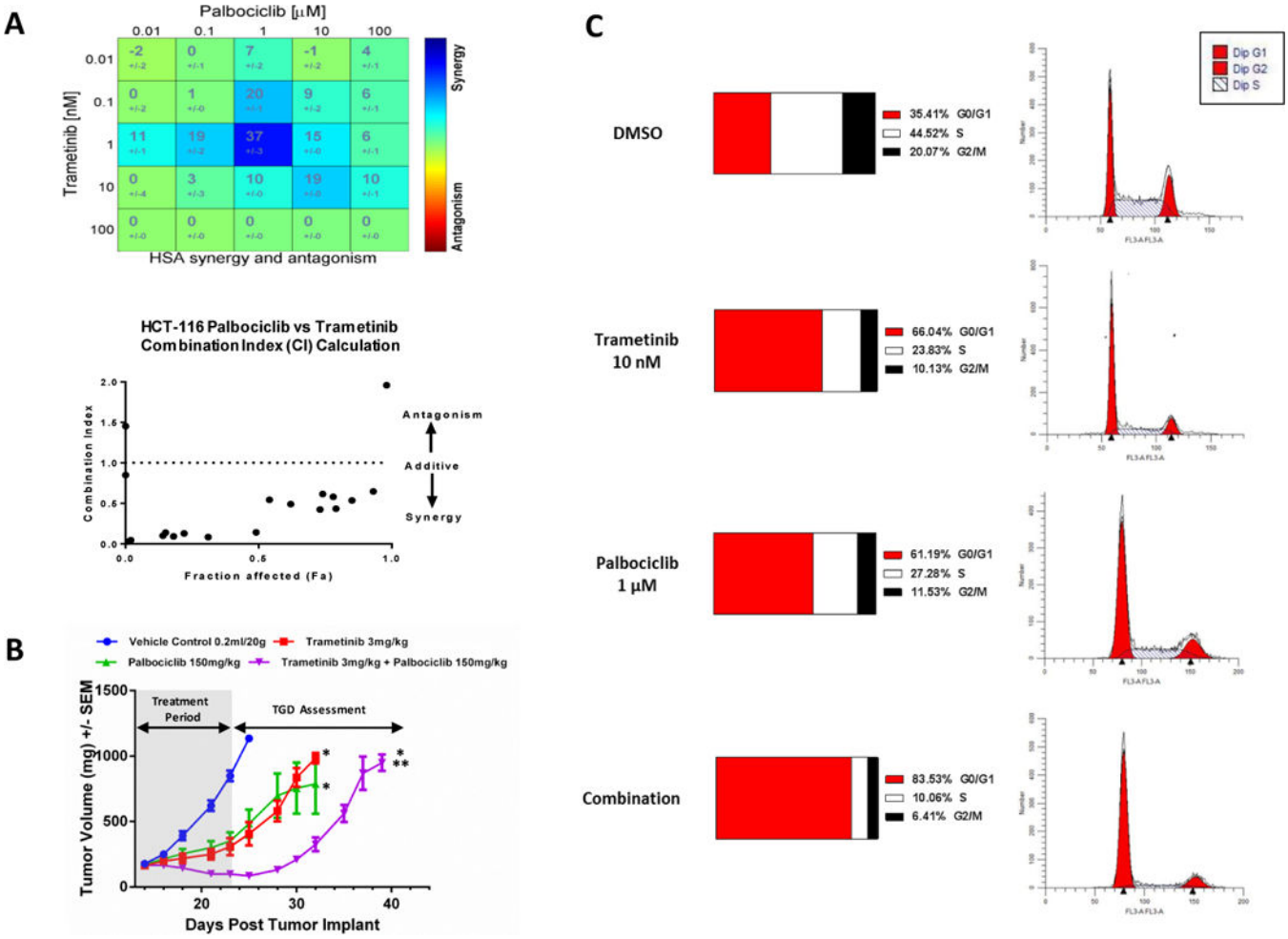

Figure 1.

In vitro and *in vivo* testing for activity against HCT-116. (**A**) Heatmap of Loewe synergy and antagonism shows the amount of additional activity achieved by a particular combination dose based on the single agent response predictions (top panel) and plot depicting the distribution of synergy scores across the matrix of combination doses using the Combination Index calculation (bottom panel). (**B**) Combination activity of trametinib and palbociclib against subcutaneous HCT-116 tumors (n=5 per group). Animals were dosed daily PO for ten consecutive days as indicated in the legend. Statistical analysis: * indicates $p<0.001$ compared to the vehicle control arm. ** indicates $p=0.001$ and $p=0.002$ compared to the trametinib and palbociclib arms, respectively. (**C**) Quantitative flow cytometry analysis of cell cycle distribution in HCT-116 cells treated with DMSO, trametinib (1 nM), palbociclib (1 μM), or the combination showing increased G1 arrest with combination treatment.

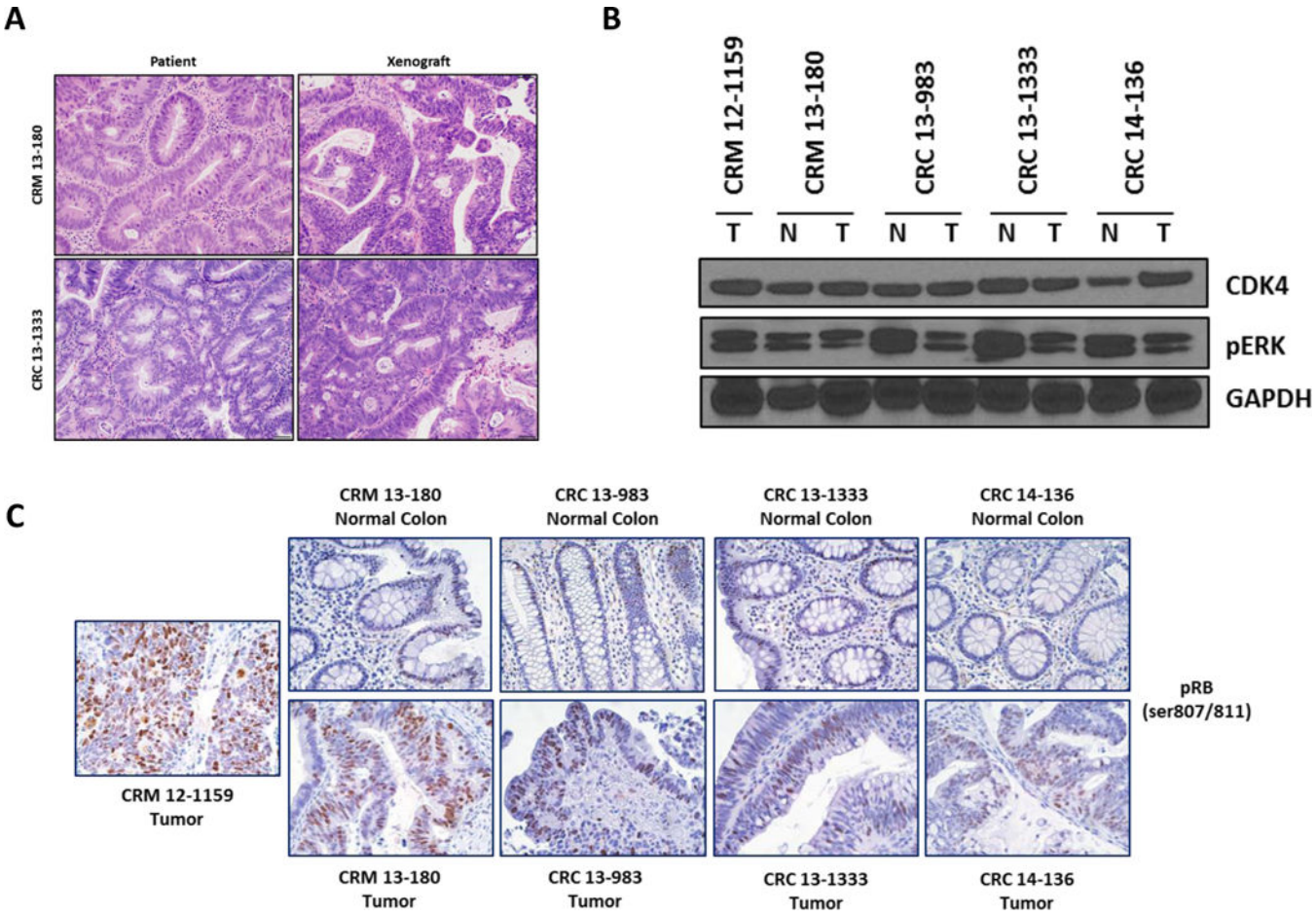

Figure 2.

Development and characterization of a panel of CRC PDX models. (**A**) Histology of representative primary tumor xenografts and the patient tumor from which they were derived. (**B**) CDK4 and pERK expression in five individual colorectal cancer PDX models (T) and matched normal colon mucosa (N). Normal colon mucosa was not obtained from the patient for the tumor represented in lane 1 (CRM 12-1159). (C) IHC staining for pRB expression in five CRC PDX tumors and matched normal colon mucosa.

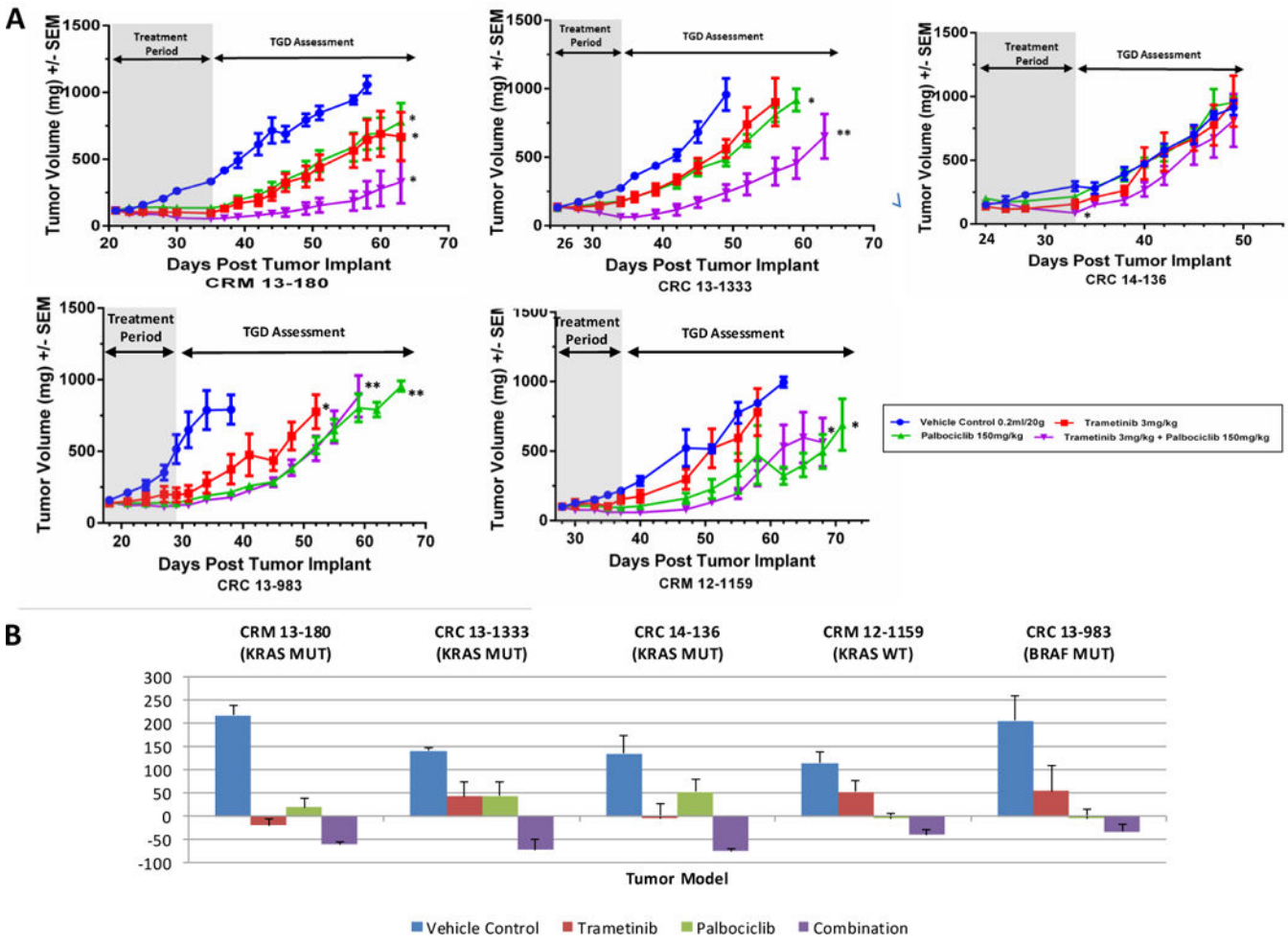

Figure 3.

Comparison of the efficacy of trametinib or palbociclib as monotherapy and combination therapy in five CRC PDX models. Trametinib and palbociclib were administered by oral gavage at 3 mg/kg and 150 mg/kg, respectively, alone or in combination. Following completion of treatment, the mice were held for a tumor growth delay assessment. (Top left) Mean tumor growth rate as a result of 12 days of treatment in CRM 13-180 (n = 5 per group). * indicates p = 0.002 compared to the vehicle control arm. (Top middle) Mean tumor growth rate as a result of 10 days of treatment in CRC 13-1333 (n = 4 per group). * indicates p = 0.006 compared to the vehicle control arm. ** indicates p < 0.001, p = 0–002, p = 0.001 compared to the vehicle control, trametinib, and palbcociclib arms, respectively. (Top right) Mean tumor growth rate as a result of 10 days of treatment in CRC 14-136 (n = 3 per group). * indicates tumor burden on last day of treatment was significantly different compared to control arm (p < 0.001 and palbociclib (p = 0.002). (Bottom left) Mean tumor growth rate as a result of 10 days of treatment in CRC 13-983 (n = 4 per group). * indicates p = 0.008 compared to the vehicle control. ** indicates p < 0.001, compared to the vehicle control, palbociclib, and combination arms, respectively. (Bottom middle) Mean tumor growth rate as a result of 10 days of treatment in CRM 12-1159 (n = 5 per group). * indicates p = 0.005 compared to the vehicle control. (B) Waterfall plot depicting the effects

of monotherapy versus combination therapy in five CRC PDX models. Values were normalized against tumor volume at baseline (beginning of treatment).

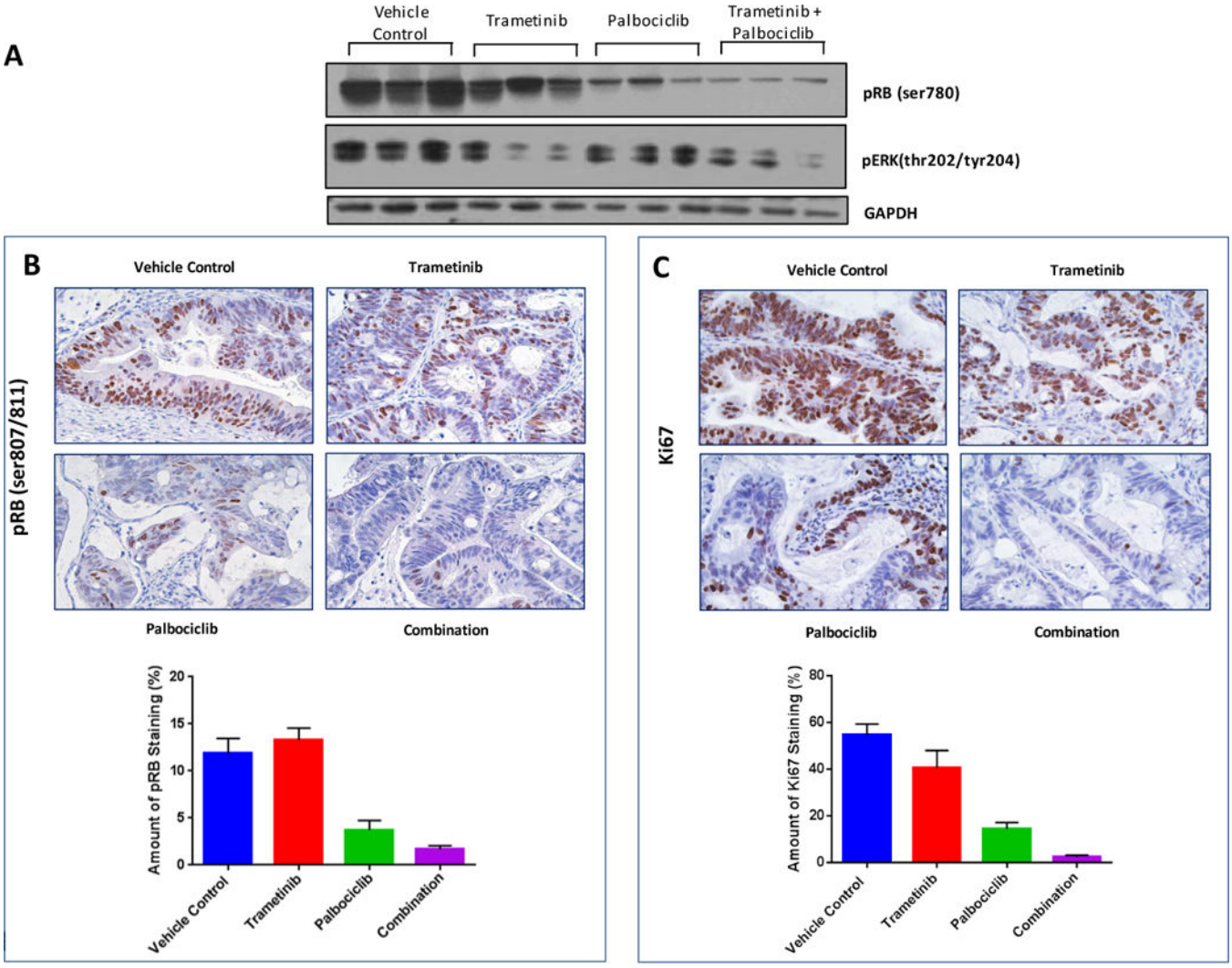

Figure 4.

(A) Immunoblot analysis of pRB (ser780) and pERK (thr202/tyr204) in CRM 13-180 tumors harvested from the efficacy experiment. Tumors were harvested at two hours following the last treatment, lysed and probed with the indicated antibodies. (B) Immunohistochemical staining of pRB in CRM 13-180 tumors. A subsequent study (no efficacy component) was carried out to generate additional tumors for IHC analysis. Mice bearing subcutaneous CRM 13-180 tumors were treated by oral gavage for 10 days with vehicle, trametinib at 3mg/kg, palbociclib at 150mg/kg, or the combination at the single agent doses. Tumors were harvested at two hours following the last treatment. Tumors were stained for pRB (ser807/811) expression (top) and the amount of staining was quantitated. (C) Tumors were also stained for Ki67 (top) and the amount of staining was quantitated (bottom). $P = 0.0191$ (vehicle versus trametinib) and $p \leq 0.0001$ for all other group comparisons.

Table 1

Clinical and pathological features of five colorectal cancer patients.

Model	Gender	Age	Prior Chemotherapy	Location	Histopathology				Mutational Status					p16 Methylation Status	Microsatellite Instability Status
					Type	TNM	Stage	Degree of Tumor Differentiation (Grade)	KRAS	BRAF	PIK3CA	APC	TP53		
UM-CRM 12-1159	M	51	Unkn	Liver	ADC	Unkn	Unkn	Moderate	WT	WT	**H1047R**	WT	**p.Y102C**	Unkn	Unkn
UM-CRM 13-180	F	72	No	Left ovary	ADC	pT3N1aM1a	IVA	Moderate	**G12V**	WT	WT	WT	**p.R248W**	Unmethylated	MSS
UM-CRC 13-983	F	69	No	Right/Left colon	ADC	pT3N1c	IIIB	Moderate	WT	**V600E**	WT	Unkn	**p.A6V**	Methylated	**MSI**
UM-CRC 13-1333	F	53	No	Sigmoid colon	ADC	pT3N1b	IIIB	Moderate	**G12D**	WT	**Q546L**	**p.R1432X**	WT	Unmethylated	MSS
UM-CRC 14-136	M	54	No	Right colon	MUC	pT3N0	IIA	Moderate	**Q61H**	WT	**E542K**	Unkn	Unkn	Unmethylated	MSS

Abbreviations: ADC = Adenocarcinoma; MSI = Microsatellite instable; MSS = Microsatellite stable; MUC = mucinous; Unkn = Unknown; WT = Wild type

Table 2

Comparison of the efficacy of monotherapy and combination therapy in five CRC PDX models. T/C represents the relative size of the median tumor burden of the treated versus vehicle control groups on the last day of treatment. Tumor growth delay (T-C) represents the difference in days for the treated (T) and vehicle control (C) tumor burden to reach a median size of 750 mg.

Model	Mutational Status	Trametinib				Palbocicilb				Trametinib + Palbociclib			
		T/C (%)	T-C (days)	PR (%)	CR (%)	T/C (%)	T-C (days)	PR (%)	CR (%)	T/C (%)	T-C (days)	PR (%)	CR (%)
CRM 13-80	KRAS (G12V)	28	13	20	0	39	15	0	0	20	>90	80	0
CRC 13-1333	KRAS (G12D) PIK3CA (Q546L)	64	5	0	0	68	8	0	0	30	19	25	25
CRC 14-136	KRAS (Q61H) PIKCA (E542K)	43	2	0	0	61	0	0	0	25	5	66	0
CRM 12-1159	PIK3CA (H1047R)	72	3	0	0	45	16	0	0	28	16	40	0
CRC 13-983	BRAF (V600E)	38	19	0	0	27	25	0	0	24	23	0	0